Interface effects in the Ni 2*p* x-ray photoelectron spectra of NiO thin films grown on oxide substrates

I. Preda and A. Gutiérrez
Departamento de Física Aplicada e Instituto de Ciencia de Materiales Nicolás Cabrera, Universidad Autónoma de Madrid, Cantoblanco, 28049 Madrid, Spain

M. Abbate
Departamento de Física, Universidade Federal do Paraná, Caixa Postal 19081, 81531-990 Curitiba, Paraná, Brazil

F. Yubero
Instituto de Ciencia de Materiales de Sevilla (CSIC), Universidad de Sevilla, Avenida Américo Vespucio s/n, 41092 Sevilla, Spain

J. Méndez and L. Alvarez
Instituto de Ciencia de Materiales de Madrid (CSIC), Cantoblanco, 28049 Madrid, Spain

L. Soriano
Departamento de Física Aplicada e Instituto de Ciencia de Materiales Nicolás Cabrera, Universidad Autónoma de Madrid, Cantoblanco, 28049 Madrid, Spain

(Received 6 September 2007; revised manuscript received 20 November 2007; published 13 February 2008)

We report the Ni 2*p* x-ray photoelectron spectra of NiO thin films grown on different oxide substrates, namely, SiO_2, Al_2O_3, and MgO. The main line of the Ni 2*p* spectra is attributed to the bulk component, and the shoulder at 1.5 eV higher binding energies to the surface component. The spectra of the NiO thin films show strong differences with respect to that of bulk NiO. The energy separation between the main peak and the shoulder increases with the substrate covalence. This indicates the strong covalent interactions between the NiO thin films and the oxide substrates, and reflects changes in the bonding at the interface from a more ionic to a more covalent interaction. These conclusions are supported by cluster model calculations with a reduced O 2*p*-Ni 3*d* hybridization.

DOI: 10.1103/PhysRevB.77.075411 PACS number(s): 73.20.−r, 79.60.Jv, 72.80.Ga

I. INTRODUCTION

The main aim of this work is to study the electronic structure of the interfaces formed by the deposition of NiO thin films on selected oxides, namely, SiO_2, Al_2O_3, and MgO. The experimental technique used in the study was Ni 2*p* x-ray photoelectron (XPS) spectra. Recent results on the electronic structure of nanostructured NiO have shown that the lower symmetry at the NiO surface produces a splitting of the unoccupied e_g states, as observed by means of the O 1*s* x-ray absorption (XAS).[1] Besides, it has also been shown that the contribution to the Ni 2*p* XPS spectrum of the pyramidaly coordinated Ni atoms located at the NiO surface overlaps with the known shoulder at 1.5 eV higher binding energy from the main line in the Ni 2*p* XPS spectra of NiO,[2] thus giving an important surface contribution to the shoulder. These results open up a different scope in the interpretation of the Ni 2*p* XPS spectra in nanoscopic systems such as NiO/oxide interfaces. By taking advantage of the above interpretations, we show below that the Ni 2*p* XPS spectra of the NiO/oxide interfaces formed at very low NiO coverage on the selected oxide not only contain a strong interface character, but also reflect the influence of the covalent bonding at the interface.

NiO is a very interesting material and its electronic structure has been controversial for years. Its electronic structure gives rise not only to interesting catalytic and magnetic properties, but also to complex line-shape spectra, in particular, in photoemission. NiO is a $3d^8$ charge transfer oxide where the ground state is a mixture of $3d^8+3d^9\underline{L}+3d^{10}\underline{L}^2$ states.[3–5] Accordingly, the final state of the Ni 2*p* photoemission spectrum of NiO shows three peaks labeled as $\underline{c}3d^8$, $\underline{c}3d^9\underline{L}$, and $\underline{c}3d^{10}\underline{L}^2$ in Fig. 1. The spectrum presents a shoulder shifted 1.5 eV toward higher binding energies from the main line, whose interpretation is still controversial. Indeed, this additional peak has been assigned to many different final states in the literature. Nowadays, the most accepted interpretation of this shoulder is that it is due to a nonlocal screening process from neighbors in a Ni_7O_{36} cluster.[6] This model explains several experiments involving $Ni_xMg_{1-x}O$ and NiO/MgO systems,[7–9] but, in turn, does not explain the absence of the shoulder in the Ni 2*p* XPS spectrum of La_2NiO_4, which corresponds to a purely octahedral Ni compound.[10] However, as mentioned above, recent experimental results on NiO surfaces have provided important keys in the interpretation of the Ni 2*p* XPS spectra. Whereas the main line intensity comes from the Ni atoms octahedrally coordinated in the bulk, part of the intensity of the shoulder, labeled Surface +Non-Local in Fig. 1, comes from the pyramidally coordinated Ni atoms at the NiO surface.[2] This surface effect has been explained in terms of cluster model calculations with reduced symmetry in which the $\underline{c}3d^9\underline{L}$ line calculated for a NiO_5 cluster (pyramidal symmetry) shifts by 1 eV to higher binding energies with respect to the same line calculated for

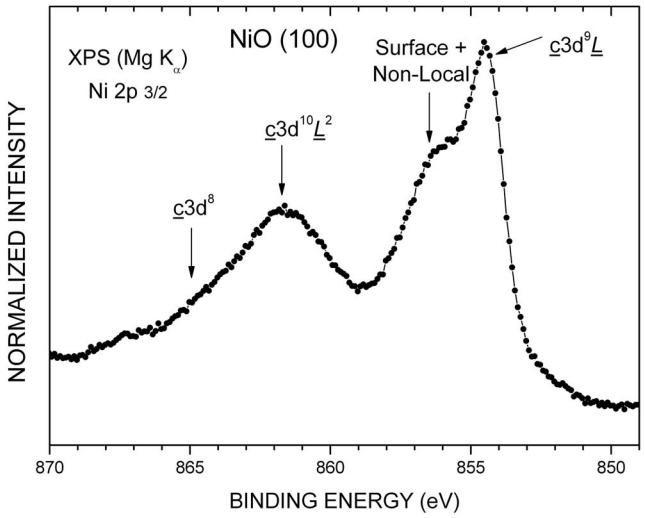

FIG. 1. Ni $2p_{3/2}$ XPS spectrum of a NiO (100) single crystal taken with 10 eV pass energy. The arrows indicate the different structures of the spectrum. For explanation, see text.

a NiO_6 cluster (octahedral symmetry). The reduced symmetry model also predicts a splitting of the unoccupied Ni e_g states at the NiO surface.[1] As we show below, the interpretation of the experimental Ni $2p$ XPS spectra of the NiO/oxide interfaces presented here is completely consistent with the above results.

Oxide thin films have become key materials in many technological applications such as catalysis, magnetic supports, materials with unique mechanical and thermal properties, sensors, etc. In all these applications, the control of the growth of the thin films is of extreme importance. In particular, the knowledge of the mechanisms influencing the growth at the interface could lead to the control of the thin film final properties. Therefore, the study of oxide/oxide interfaces seems to be well justified. In spite of this impact, studies on oxide/oxide interfaces have been scarce in the literature until the appearance of several works on oxide surfaces in the early 1990s.[11–14] In these works, the authors proposed the growth of thin oxide films on a conductive support in order to avoid charging problems during the characterization of the oxides. Since then, many works on oxide thin films have been done using different characterization techniques, in particular, x-ray and electron spectroscopies.[15] NiO/oxide systems have been extensively studied, but mainly related to the preparation of supported catalysts.[16–18] In particular, the growth of thin NiO films on MgO has been studied in more detail.[9,19–23] NiO has been found to grow epitaxially on MgO (100) single crystal. Studies on the electronic structure by XPS during the growth process of NiO on MgO (100) show that for a coverage of 1 ML, the main line of the Ni $2p$ XPS spectra is narrowed and slightly shifted to higher binding energies. In one of the studies, this effect was explained in terms of nonlocal screening,[9] whereas in another work, this peak was assigned to the $\underline{c}3d^9$-$3d$ (where $3d$ stands for a hole in the Ni $3d$ orbitals) final state configuration.[20] Structural studies on NiO grown on MgO (001) show that, initially, the overlayer NiO lattice grows coherently until a critical thickness of 60 nm is reached, at which relaxation of the NiO lattice occurs.[22] On the other hand, the work of Warot *et al.*[23] shows that NiO grows forming different nanostructures depending on the MgO surface orientation, giving wires for MgO (110) and tetrahedrons for MgO (111).

In the work presented here, the oxide substrates have been prepared as thin films following different conventional methods on conductive supports. We have to note that these substrates do not present a long range order being polycrystalline. In spite of that, a lot of important information can be extracted from the Ni $2p$ XPS spectra of these nonordered systems. The oxide substrates (SiO_2, Al_2O_3, and MgO) have been chosen according to the nature of their chemical bonding (from a more covalent to a more ionic character). Interesting trends in terms of covalency-ionicity of the substrates have already been observed by us in the study of the electronic structure of TiO_2/oxide interfaces with synchrotron radiation spectroscopies.[24,25]

II. EXPERIMENTAL DETAILS

NiO has been progressively grown on the corresponding oxide, paying special attention to the early stages of growth for very low coverage. At these stages, the effect of the substrate can be clearly observed. Successive evaporations were followed by the measurement of the XPS spectra. NiO was grown on the substrates by reactive thermal evaporation of Ni at room temperature in an oxygen atmosphere of 1×10^{-5} mbar. The evaporation rate was kept low enough to allow the study of the early stages of growth in detail. As mentioned above, we have used thin films of the oxides prepared on conductive materials and following conventional methods as substrates. The silica substrate consisted of a 200 Å thin film of amorphous SiO_2 grown by dry oxidation of a p-doped Si (111) wafer. The Al_2O_3 substrate was an ultrathin film, about 25 Å thick, grown by thermal oxidation of a pure polycrystalline Al foil at 350 °C for 30 min. MgO was deposited on a p-doped Si (111) wafer by reactive evaporation of Mg at room temperature. The quality of the substrates was previously checked by XPS and did not show any appreciable contamination. The coverage and thickness of the NiO deposits was determined by quantitative analysis of the XPS inelastic peak shape following the method described by Tougaard by means of the QUASES software.[26] A bulk NiO reference sample was also grown on a highly oriented pyrolytic graphite (HOPG) substrate using the above method and then annealed at 400 °C for 30 min in an oxygen atmosphere (1×10^{-5} mbar). It has been shown elsewhere[27] that with this method, a stoichiometric NiO thin film can be grown on HOPG.

The XPS measurements were performed using a CLAM4 electron energy analyzer and a Mg $K\alpha$ x-ray source from Thermo-Scientific. The pass energy was set to 20 eV in order to have an acceptable count rate with a reasonable energy resolution, except for the spectrum of the NiO single-crystal shown in Fig. 1, where the pass energy was set to 10 eV. The survey and core level spectra from the NiO deposits were measured for quantitative and qualitative analyses. A Shirley background was removed from the Ni $2p$ XPS spectra by

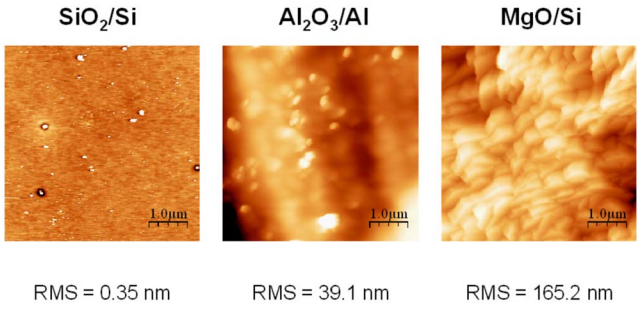

FIG. 2. (Color online) AFM topographic images (5×5 μm^2) of the different oxide surfaces measured in dynamic mode (tapping). rms (root mean square) roughness values are given for comparison.

using a conventional software. Since charging of the sample was progressively increasing with the successive evaporations, an absolute energy calibration for all series of spectra was difficult to perform. Thus, the spectra were calibrated using the main line of the Ni 2*p* XPS spectrum of NiO at 854.5 eV binding energy. Atomic force microscope (AFM) images were measured in dynamic mode (tapping) using Nanotec's microscope and software.[28]

III. RESULTS AND DISCUSSION

The AFM images of the three substrates are shown in Fig. 2. The silicon oxide shows flat areas with a few contaminants, some of them, prior to the oxide growth, produce a small depression in the oxide around. The roughness is less than half a nanometer as expected from the oxidation of a polished Si single crystal. The Al_2O_3 oxide has an intermediate roughness of 39 nm, which is consistent with the roughness of an oxidized Al polycrystalline sheet. The largest value of the rms roughness corresponds to the MgO substrate (165 nm). The relatively large roughness for the MgO substrate is produced by the formation of faceted crystallites of about 1 μm size.

The Ni $2p_{3/2}$ XPS spectra for large NiO coverages, approximately 100 equivalent monolayers (ML), on the corresponding oxide substrates are shown in Fig. 3. We have also included the bulk NiO reference spectrum, in Fig. 3(a), for comparison purposes. In general, all the spectra have the same structures observed in the spectrum of the NiO single crystal shown in Fig. 1, although this was measured with a higher energy resolution. In order to analyze the peak intensities, we have fitted the spectra using three conventional curves: one for the main line at 854.5 eV, another for the shoulder at 856.0 eV, and a third one to simulate the charge-transfer satellite at 861.5 eV. It is worth noting that although, according to the literature, the shoulder is separated by 1.5 eV from the main line, our fittings give a broad Lorentzian-like peak with intensity ratio of $I_{sat}/I_{main}=1.97$, and separated by 1.72 eV from the main line for the shoulder of the NiO single crystal (Fig. 1). For the spectrum of the NiO thin film shown in Fig. 3(a), the intensity ratio is 2.44 eV and the energy separation is 1.83 eV. This small disagreement can be related to the lack of long range order in

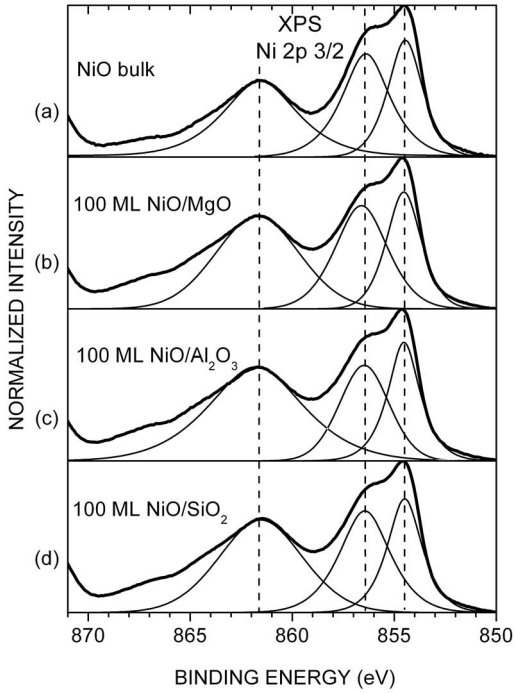

FIG. 3. (a) Ni $2p_{3/2}$ XPS spectrum of a 200 Å NiO thin film grown on highly oriented pyrolitic graphite, used as bulk NiO reference. (b)–(d) Ni $2p_{3/2}$ XPS spectrum of NiO thin films about 100 equivalent monolayers thick, grown on the different oxide substrates.

the NiO thin film. Further, the NiO thin film has a larger effective surface than the NiO single crystal so that, according to the model suggested in Ref. 2, the surface component should be slightly higher. The broad line shape of the shoulder (2.85 eV) is consistent with a model in which the contributions of nonlocal and surface effects to the Ni 2*p* XPS spectra overlap in the energy region of the shoulder. Finally, since all the spectra of the NiO thin films grown on the oxide substrates in Fig. 3 are almost identical, we can conclude that a stoichiometric NiO thin film can be grown on any of the selected oxide substrates, and shows the same electronic structure as bulk NiO.

The most important features of the experiment appear for a very low coverage. Figure 4 shows the Ni $2p_{3/2}$ XPS spectra of the early stages of growth (0.5–0.8 ML) of NiO on the different oxide substrates. The spectrum of bulk NiO, in Fig. 4(a), was also included for comparison. In this case, the spectra of the NiO submonolayers do not match the spectrum of bulk NiO. The spectra for the MgO and Al_2O_3 substrates show that the main line is formed by a broad single peak instead of a double peak, whereas the spectrum for the SiO_2 substrate presents the double peak, but the relative intensity of the shoulder is much higher than for the bulk spectrum. We have to note that the spectrum of the NiO submonolayer grown on the MgO substrate agrees perfectly with the other spectra reported in the literature for this system.[9,20] If one looks at the fittings for the MgO and Al_2O_3 substrates in Fig. 4, it can be observed that both the main line and the shoulder are present in the spectra, but in theses cases the shoulder has a much higher intensity with respect to bulk NiO. These

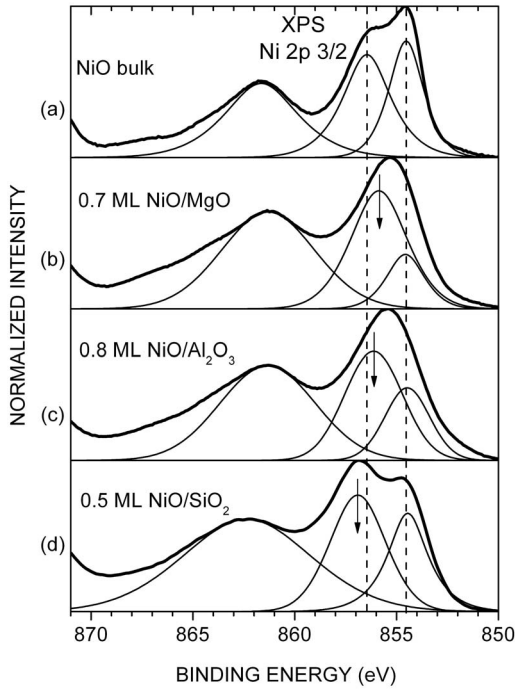

FIG. 4. (a) Ni $2p_{3/2}$ XPS spectrum of a 200 Å NiO thin film grown on highly oriented pyrolitic graphite, used as bulk NiO reference. (b)–(d) Ni $2p_{3/2}$ XPS spectrum of NiO submonolayers (0.3–0.8 ML) grown on the different oxide substrates.

results agree with the idea that the shoulder comes mostly from the pyramidally coordinated Ni atoms at the surface of these nanostructured systems.

As mentioned above, we have performed quantitative analysis of the first stages of NiO growth on SiO_2, Al_2O_3, and MgO by means of XPS inelastic peak shape analysis. As a first conclusion, the results in Fig. 5 reflect that the way of growth of NiO on all the substrates studied here is through

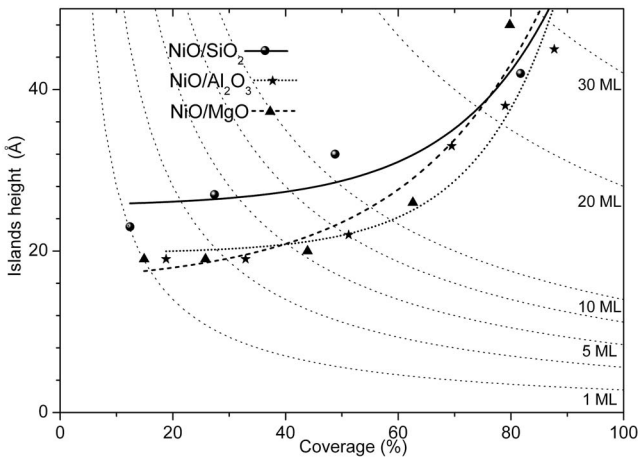

FIG. 5. Quantitative analysis (average particle height versus surface coverage) of the first stages of NiO growth on SiO_2 (dots), Al_2O_3 (stars), and MgO (triangles) by means of XPS inelastic peak shape analysis using QUASES software (Ref. 19). Dashed lines indicate equivalent amount of NiO deposited material.

the Stransky-Krastanov-like mode, i.e., growth of small islands of a determined height at the early stages of growth. This is in contrast to the layer-by-layer growth found for a MgO (100) single crystal. However, it can be explained as due to the formation of many nucleation centers at the grain boundaries of the polycrystalline material. The results suggest that small NiO aggregates (size below 22 Å) are formed on either substrate for equivalent NiO amount deposited below 1 ML. Therefore, it seems reasonable that the Ni $2p$ XPS spectra of these nanostructured NiO systems are dominated by the surface component, i.e., the shoulder. If we assume that the bulk component is directly related to the amount of octahedrally coordinated Ni atoms, its intensity should be proportional to the height of the NiO aggregates for each substrate. Indeed, this is also in agreement with the quantitative analysis shown in Fig. 5. Even taking into account the errors given by the calculation method[29] and considering that the fittings are only an approach to the proposed model, it seems clear that larger NiO aggregates are formed on SiO_2 than on the other two substrates for the same equivalent NiO material on each substrate. Thus, for 1 ML NiO deposited on SiO_2, the NiO aggregates can be considered of about 22 Å size, covering 12% of the surface, while on Al_2O_3 and MgO, their sizes are 15%–20% smaller. The bulk component of the fittings presented in Fig. 4 clearly shows this trend.

Another interesting feature of the spectra shown in Fig. 4 is that the energy shift of the two components, main line and shoulder, is not constant throughout the series of spectra. In fact, the highest energy separation is obtained for the SiO_2 substrate (2.5 eV), whereas the lowest (1.3 eV) is found for the MgO substrate, and an intermediate value (1.7 eV) is observed for the Al_2O_3 substrate. It is surprising that the energy separation between the bulk and surface components for the SiO_2 substrate is even higher than for bulk NiO (1.9 eV), whereas for the Al_2O_3 and MgO substrates, these values are lower than for bulk NiO.

To understand this effect, we performed cluster model calculations of the Ni $2p$ XPS spectra. Starting from a NiO_6 cluster, the Ni $3d$-O $2p$ overlap of the apical O atoms were progressively reduced ($T_{\text{apical}}/T_{\text{basal}}=1$ corresponds to octahedral symmetry, 0.66 to pyramidal symmetry, and 0.33 to square planar symmetry). The ground state in the calculations was expanded in the $3d^8$, $3d^9\underline{L}$, and $3d^{10}\underline{L}^2$ configurations, where $\underline{L}$ denotes a symmetry adapted O $2p$ hole.[30] The final state was expanded in the $\underline{c}3d^8$, $\underline{c}3d^9\underline{L}$, and $\underline{c}3d^{10}\underline{L}^2$ configurations, where $\underline{c}$ here denotes a hole in Ni $2p$ core level. The Ni $2p$ photoelectron spectra were then calculated using the sudden approximation.[18]

The parameters used in the cluster model calculation were the charge-transfer energy Δ, the Mott-Hubbard repulsion U, the core-hole potential Q, and the p-d transfer integral $(pd\sigma)$.[31] The multiplet splitting was obtained in terms of the Raccah parameters (B,C) and the crystal-field splitting $10Dq$. The transfer of the x^2-y^2 electron involved T_{basal}, whereas the transfer of the z^2 level involved T_{apical}.[32] A summary of the parameters used in the calculations is given in Table I.

The results of the calculations are shown in Fig. 6, where the calculated Ni $2p$ XPS spectra are given as a function of

TABLE I. Parameters used in the cluster model calculation of the Ni 2*p* XPS spectra: charge transfer energy (Δ), Mott-Hubbard repulsion (U), *p-d* transfer integral ($pd\sigma$), core-hole potential (Q), *d-d* Racah parameters (B,C), and crystal-field splitting $10Dq$.

Main parameters	
U	7.5
Δ	4.0
$pd\sigma$	1.5
Q	9.0
Multiplet parameters	
B	0.13
C	0.58
$10Dq$	0.1

T_{apical}/T_{basal} ratio. As noted above, $T_{apical}/T_{basal}=1$ corresponds to octahedral symmetry, 0.66 to pyramidal symmetry, and 0.33 to square planar symmetry. For the bulk NiO_6 cluster, the calculation presents the standard $\underline{c}3d^9\underline{L}$, $\underline{c}3d^{10}\underline{L}^2$, and $\underline{c}3d^8$ peaks. For the surface NiO_5 cluster, the calculations show these peaks, but with smaller energy spread and an additional peak in the spectrum, due to the different hybridizations of the x^2-y^2 and z^2 levels. The $\underline{c}3d^9\underline{L}$ peak has shifted by 1 eV from its value in octahedral symmetry, thus

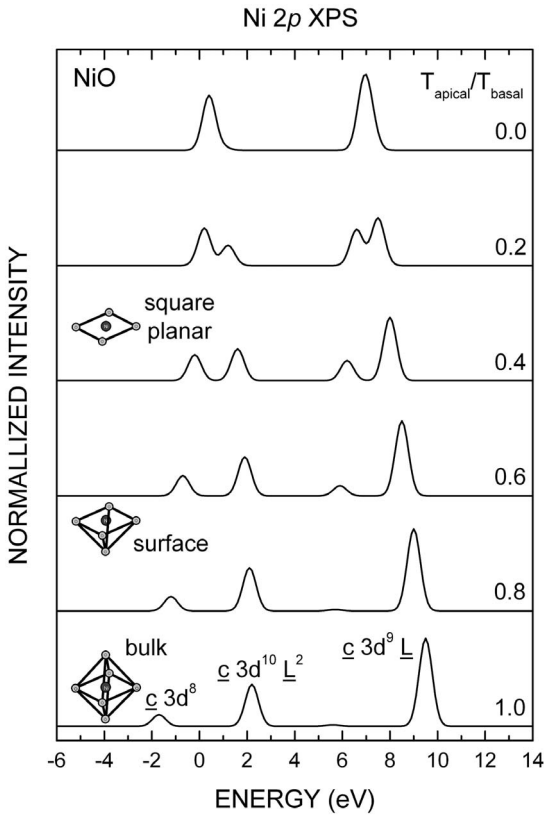

FIG. 6. Cluster model calculations of the Ni 2*p* XPS spectra as a function of the ratio T_{apical}/T_{basal} (1.0 corresponds to octahedral symmetry, 0.66 corresponds to pyramidal symmetry, and 0.33 to square planar symmetry).

contributing to the shoulder intensity. The overall energy separation between the peaks is roughly given by $\Delta E^2=(Q-\Delta)^2+4T_{eff}^2$. Therefore, the smaller energy spread above is attributed to the reduced T_{eff} in pyramidal symmetry.

The results of the calculations show that the main component of the Ni 2*p* XPS spectra comes from the octahedrally coordinated Ni atoms in the bulk, whereas the pyramidally coordinated atoms at the surface contribute at the shoulder energy, shifted around 1 eV. A further symmetry reduction (or a further covalence reduction) would produce an even larger shift. These results also help to explain our experimental results on the NiO overlayers on the different oxides.

According to the above calculations, the energy separation of the bulk (main line) and surface (shoulder) peaks decreases with the T_{apical}/T_{basal} ratio. This separation is related to the changes in the covalent interaction at the NiO/oxide interface, being larger for the NiO overlayer on the more covalent SiO_2 substrate and smaller in the more ionic MgO substrate. These results are consistent with the formation of Ni-O-M cross-linking bonds (M=Si, Al, and Mg) at the interface. In this picture, in the case of the SiO_2 substrate, the Ni 3*d*-O 2*p* overlap in the Ni-O-Si bonds is smaller than in the Ni-O-Ni bonds of bulk NiO due to the strong covalent character of the Si-O bonding. On the other hand, the Ni 3*d*-O 2*p* overlap of the Ni-O-Mg bonds is larger than in the Ni-O-Ni bonds due to the more ionic character of the Mg-O bonds.

The above results have been successfully interpreted in terms of the surface and bulk components of the Ni 2*p* XPS spectra according to the model proposed in Ref. 2. This model, as mentioned above, suggests that the shoulder has an important surface character, but the nonlocal effects cannot be neglected. However, in this work, the interpretation of the experimental results has been done in terms of surface and bulk components, corresponding to the shoulder and main component, respectively, of the Ni 2*p* XPS spectra. This is due to the nanostructured character and the high surface to volume ratio of the systems analyzed here. Thus, this model seems to be a suitable tool for the interpretation of the Ni 2*p* XPS spectra in NiO nanostructures.

In the following, we are going to explore the influence of other possible effects, such as quantum-size and structural effects. In the study of the similar TiO_2/SiO_2 system, Lassaleta *et al.*[33] found an increase of the band gap for very low coverages. They attributed this shift to a combination of quantum-size and interface (cross-linking bonds) effects, however they pointed out that, in this case, the nature of the substrate is more important than the layer thickness. In our case, the Ni LMV Auger spectra for NiO grown on all substrates (not shown here) do not reveal any apparent energy shift. On the contrary, they also reflect a peak narrowing as in the case of the Ni 2*p* XPS spectra and are in complete agreement with the spectra reported by Sanz and Tyliev[20] for the growth of NiO on MgO (100). Therefore, quantum-size effects do not seem to play a significant role in the deposits studied in this work. The influence of structural effects in the Ni 2*p* XPS spectra should also be evaluated. For instance, Warot *et al.*[23] found that the surface morphology of the NiO overlayer depends on the surface orientation in different MgO single-crystal substrates. In our case, the AFM images

of the MgO substrate shown in Fig. 2 indicate the formation of faceted crystallites of about 1 μm with a random orientation. However, the fact that our spectra on these polycrystalline substrates completely match those obtained on MgO (100) single crystals[9,6] indicates that surface orientation is not a dominant effect in this work. Other structural effects such as interface mixing, as well as geometry and lattice mismatch, could also be influencing the spectra. As pointed out by Towler *et al.*,[30] small changes in the surface geometry can lead to significant effects on the initial states of the ions in oxide materials. Indeed, significant variations of the crystal field of the Ti atoms located at the TiO_2/SiO_2 system have been observed by us by means of the Ti $2p$ XAS spectra.[24] However, these changes have also been explained in terms of a covalence reduction due to the different environment of the Ti atoms. Unfortunately, no data on the coordination of the Ni atoms at these NiO/oxide interfaces are available at the moment. However, the XPS spectra presented in this work are consistent with an octahedral coordination surrounded by a mixture of Ni and M atoms (M=Si, Al, and Mg) in the second coordination sphere and are supported by their resemblance with other published spectra. In this picture, the effect of cation intermixing and small lattice parameter variations due to the lattice mismatch would not change the conclusions of this work.

IV. CONCLUSIONS

In summary, we studied the electronic structure of selected NiO/oxide interfaces using the Ni $2p$ XPS spectra. The main peak in the spectra is related to the bulk component, whereas the shoulder corresponds to the surface component. For submonolayer NiO coverage, the spectra are dominated by the surface component, as expected. On the other hand, the bulk component in the spectra increases for larger NiO coverage. The energy separation between the surface and bulk components scales with the covalence of the substrate. This effect indicates a strong interaction of the NiO layers with the covalent substrates. The experimental trends can be understood using cluster model calculations of the Ni $2p$ XPS spectra. This demonstrates that this approach is a useful tool in the study of nanostructured NiO systems.

ACKNOWLEDGMENTS

We would like to thank G. A. Sawatzky for useful comments and suggestions. We want to thank the support of the MECD of Spain under Contracts No. FIS2006-06240 and No. MAT2007-66719-C03-03, and the Comunidad de Madrid under Contract No. CCG06-UAM/MAT-0227.

[1] L. Soriano, A. Gutiérrez, I. Preda, S. Palacín, J. M. Sanz, M. Abbate, J. F. Trigo, A. Vollmer, and P. R. Bressler, Phys. Rev. B **74**, 193402 (2006).
[2] L. Soriano, I. Preda, A. Gutiérrez, S. Palacín, M. Abbate, and A. Vollmer, Phys. Rev. B **75**, 233417 (2007).
[3] A. Fujimori, F. Minami, and S. Sugano, Phys. Rev. B **29**, 5225 (1984).
[4] G. A. Sawatzky and J. W. Allen, Phys. Rev. Lett. **53**, 2339 (1984).
[5] S. Hüfner, Solid State Commun. **52**, 793 (1984).
[6] M. A. van Veenendaal and G. A. Sawatzky, Phys. Rev. Lett. **70**, 2459 (1993).
[7] P. Kuiper, G. Kruizinga, J. Ghijsen, G. A. Sawatzky, and H. Verweij, Phys. Rev. Lett. **62**, 221 (1989).
[8] M. Abbate, F. M. F. de Groot, J. C. Fuggle, A. Fujimori, Y. Tokura, Y. Fujishima, O. Strebel, M. Domke, G. Kaindl, J. van Elp, B. T. Thole, G. A. Sawatzky, M. Sacchi, and N. Tsuda, Phys. Rev. B **44**, 5419 (1991).
[9] D. Alders, F. C. Voogt, T. Hibma, and G. A. Sawatzky, Phys. Rev. B **54**, 7716 (1996).
[10] L. Sangaletti, L. E. Depero, and F. Parmigiani, Solid State Commun. **103**, 421 (1997).
[11] G. H. Vurens, M. Salmerón, and G. A. Somorjai, Prog. Surf. Sci. **32**, 333 (1990).
[12] V. E. Henrich, Prog. Surf. Sci. **50**, 77 (1995).
[13] V. E. Henrich and P. A. Cox, *The Surface Science of Metal Oxides* (Cambridge University Press, Cambridge, England, 1994), Chap. 7.
[14] R. J. Lad, Surf. Rev. Lett. **2**, 109 (1995).
[15] A. R. González-Elipe and F. Yubero, in *Handbook of Surfaces and Interfaces of Materials*, edited by H. S. Nalwa (Academic, San Diego, 2001), Chap. 4.
[16] A. Corrias, G. Mountjoy, G. Piccaluga, and S. Solinas, J. Phys. Chem. B **103**, 10081 (1999).
[17] X. J. Zhang, J. X. Liu, Y. Jing, and Y. C. Xie, Appl. Catal., A **240**, 1 (2003).
[18] M. Nurunnabi, B. T. Li, K. Kunimori, K. Suzuki, K. Fujimoto, and K. Tomishige, Catal. Lett. **103**, 277 (2005).
[19] S. D. Peacor and T. Hibma, Surf. Sci. **301**, 11 (1994).
[20] J. M. Sanz and G. Tyliev, Surf. Sci. **367**, 196 (1996).
[21] J. M. Sanz, L. Soriano, P. Prieto, G. Tyuliev, C. Morant, and E. Elizalde, Thin Solid Films **332**, 209 (1998).
[22] M. A. James and T. Hibma, Surf. Sci. **433**, 718 (1999).
[23] B. Warot, E. Snoek, J. C. Ousset, M. J. Casanove, S. Dubourg, and J. F. Bobo, Appl. Surf. Sci. **188**, 151 (2002).
[24] L. Soriano, G. G. Fuentes, C. Quirós, J. F. Trigo, J. M. Sanz, P. R. Bressler, and A. R. González-Elipe, Langmuir **16**, 7066 (2000).
[25] M. Sánchez-Agudo, L. Soriano, C. Quirós, M. Abbate, L. Roca, J. Avila, and J. M. Sanz, Langmuir **17**, 7339 (2001).
[26] S. Tougaard, QUASES, Software package for quantitative XPS/AES of surface nanostructures by inelastic peak shape analysis, see www.QUASES.com
[27] I. Preda, M. Abbate, A. Gutiérrez, S. Palacín, A. Vollmer, and L. Soriano, J. Electron Spectrosc. Relat. Phenom. **156-158**, 111 (2007).
[28] I. Horcas, R. Fernández, J. M. Gómez-Rodríguez, J. Colchero, J. Gómez-Herrero, and A. M. Baró, Rev. Sci. Instrum. **78**, 013705 (2007).
[29] S. Tougaard, Surf. Interface Anal. **26**, 249 (1998).
[30] M. D. Towler, N. M. Harrison, and M. I. McCarthy, Phys. Rev. B

52, 5375 (1995).
[31] G. van der Laan, C. Westra, C. Haas, and G. A. Sawatzky, Phys. Rev. B **23**, 4369 (1981).
[32] G. Zampieri, F. Prado, A. Caneiro, J. Briatico, M. T. Causa, M. Tovar, B. Alascio, M. Abbate, and E. Morikawa, Phys. Rev. B **58**, 3755 (1998).
[33] G. Lassaleta, A. Fernández, J. P. Espinós, and A. R. González-Elipe, J. Phys. Chem. **99**, 1484 (1995).